Review Article

Imaging of dorsal wrist pain

Alex W. H. Ng[1]^, Julianna Y. S. Chan[1]^, James F. Griffith[1]^, Isaac S. H. Ng[2]^, Wing Lim Tse[3], Sarah S. H. Ng[4]^

[1]Department of Imaging and Interventional Radiology, Prince of Wales Hospital, The Chinese University of Hong Kong, Hong Kong, China; [2]Kings College London, University of London, London, UK; [3]Department of Orthopedics and Traumatology, Prince of Wales Hospital, The Chinese University of Hong Kong, Hong Kong, China; [4]Cardiff Sixth Form College, Wales, UK

Contributions: (I) Conception and design: All authors; (II) Administrative support: AWH Ng, JYS Chan, ISH Ng, SSH Ng; (III) Provision of study materials or patients: AWH Ng, JYS Chan, JF Griffith, WL Tse; (IV) Collection and assembly of data: All authors; (V) Data analysis and interpretation: AWH Ng, JYS Chan, JF Griffith, WL Tse; (VI) Manuscript writing: All authors; (VII) Final approval of manuscript: All authors.

Correspondence to: Alex W. H. Ng, MBChB, FRCR. Department of Imaging and Interventional Radiology, Prince of Wales Hospital, The Chinese University of Hong Kong, 30-32 Ngan Shing Street, Shatin, New Territories, Hong Kong, China. Email: alex@sunghim.com.

Abstract: Pain on the dorsal side of the wrist is a common clinical presentation, comparable to pain experienced on the ulnar and radial aspects of the wrist. The dorsal wrist region has distinct anatomical features and is associated with a wide spectrum of pathologies, including conditions affecting the bones, cartilage, ligaments, and tendons. Accurate diagnosis often depends on imaging techniques such as radiographs and ultrasound, with a growing trend towards the use of magnetic resonance imaging (MRI) for more detailed assessment of complex cases. The role of imaging in diagnosing dorsal wrist pain is expected to expand further in the future. To the best of our knowledge, there has not been a comprehensive review paper that specifically addresses the imaging findings related to dorsal wrist pain. This review aims to fill that gap by discussing the imaging characteristics of both common and uncommon pathologies that can cause dorsal wrist pain. It provides an overview of the most appropriate imaging modalities to evaluate various causes of dorsal wrist pain, highlights key imaging findings, and discusses differential diagnoses. By doing so, this review seeks to enhance the understanding and interpretation of imaging results, ultimately aiding in the accurate diagnosis and management of dorsal wrist pain. This comprehensive approach underscores the critical role of advanced imaging in contemporary clinical practice.

Keywords: Dorsal wrist pain; pathology; review; imaging findings

Submitted May 03, 2024. Accepted for publication May 27, 2024. Published online Jun 13, 2024.
doi: 10.21037/qims-24-420
View this article at: https://dx.doi.org/10.21037/qims-24-420

Introduction

Dorsal wrist pain is probably at least as common a clinical presentation as ulnar- or radial-sided wrist pain. Dorsal wrist pain is often aggravated by weightbearing exercises performed with the wrists extended such as during push-ups or yoga (1). The most common pathologies identified on magnetic resonance imaging (MRI) in patients with dorsal wrist pain during wrist extension are occult dorsal wrist ganglia, scapholunate (SL) ligament injury, and dorsal capsular inflammation ('capsulitis') (2). Ultrasound, and to an even greater degree, MRI can help identify all the common and uncommon causes of dorsal wrist pain and gauge disease severity. This assessment can significantly benefit patient care.

^ ORCID: Alex W. H. Ng, 0000-0003-1268-3067; Julianna Y. S. Chan, 0000-0002-3938-4131; James F. Griffith, 0000-0001-5206-9382; Isaac S. H. Ng, 0000-0002-0323-5740; Sarah S. H. Ng, 0009-0007-0275-5027.

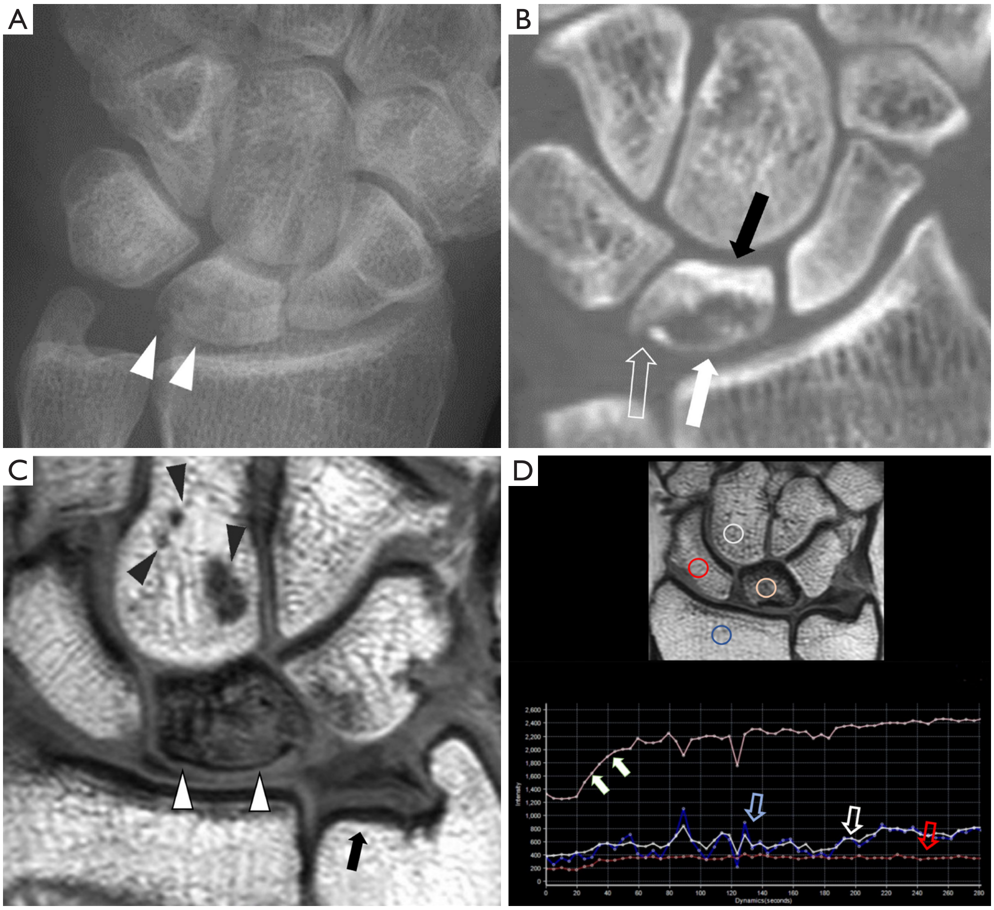

Figure 1 A 28-year-old male patient presented with dorsal wrist pain for eight months. (A) Frontal radiograph of the wrist shows mixed lytic and sclerotic changes in the lunate bone (arrowheads), predominantly at the proximal ulnar aspect of the lunate. (B) Reformatted coronal CT image shows lytic change in the proximal lunate bone with mild collapse (arrow) and cortical fracture (block arrow). The distal portion of the lunate is sclerotic (black arrow). Features are compatible with Kienbock's disease. (C) Coronal T1-weighted MR image of the same wrist shows homogeneous diffuse low signal intensity throughout the lunate (arrowheads), suggestive of loss of the fat marrow. There is ulnar negative variance (black arrow). Features are typical appearances of the AVN. The small areas of hypointensity in the capitate bone are due to subcortical cysts (black arrowheads). (D) Dynamic contrast-enhanced MRI of same wrist. Regions of interest have been put over the lunate (orange circle), distal radius (blue circle), scaphoid (red circle) and capitate (white circle). There is hyper-perfusion of the lunate with increased upslope (arrows) of the time-intensity curve compared to the normal low perfusion of the distal radius (blue block arrow), scaphoid (red block arrow) and capitate (white block arrow). This re-perfusion is thought to represent a reparative process secondary to bone ischemia. CT, computed tomography; MR, magnetic resonance; AVN, avascular necrosis; MRI, magnetic resonance imaging.

To the best of our knowledge, no review paper has discussed the imaging findings of dorsal wrist pain. This review discusses the imaging of both common and uncommon pathologies that can lead to dorsal wrist pain. The most suitable imaging examination to assess the various causes of dorsal wrist pain, pertinent imaging findings, and differential diagnosis are addressed. Bone, joint, ligament, tendon, and other soft tissue pathologies are addressed in turn.

Bone abnormality

Kienbock disease (Figure 1)

Kienbock's disease most likely results from avascular necrosis (AVN) of the lunate bone, possibly related to repetitive minor trauma. It occurs most commonly in men aged between 20 and 40, mainly in the dominant hand (3). About three-quarters of patients will have negative ulnar variance. Negative ulnar variance leads to forces being transferred from the capitate through the lunate to the radius solely rather than being dissipated to both the radius and the ulna (4). Kienbock's disease usually presents with exercise-related dorsal wrist pain, restricted flexion-extension, and diminished grip strength. Mild dorsal radiocarpal swelling and tenderness are frequently observed. Kienbock's disease is categorised into four stages based on radiographs and computed tomography (CT) (5):

- Stage 1: normal lunate density and height;
- Stage 2: mild lunate sclerosis and collapse;
- Stage 3: moderate to severe lunate collapse/fragmentation/fracture with proximal migration of capitate;
- Stage 4: secondary perilunate osteoarthritis.

Kienbocks disease commonly leads to a coronal fracture of the lunate, which splits the lunate into fairly equal-sized volar and dorsal components. This separation of the lunate, in addition to lunate collapse, leads to proximal capitate migration.

CT is better at revealing subtle lunate sclerosis and, more precisely, delineating lunate collapse and fragmentation than radiographs (6). MRI is very sensitive to identifying early Kienbock's disease through identification of bone marrow oedema (6). Typical MRI features are homogeneous low T1-weighted (T1W) signals within the lunate bone due to oedema ± fibrosis of the normal fatty marrow signal. On T2-weighted (T2W) fat-suppressed sequences, the lunate shows heterogeneous high signal intensity due to marrow oedema ± immature granulation (7). Low signal intensity on both T1W and T2W sequences signifies sclerosis or mature fibrosis, which can be discriminated by correlating the magnetic resonance (MR) findings with radiographic or CT findings. In the later stages, fibrotic and sclerotic changes within the lunate predominate over bone marrow oedema.

T1-hypointensity and T2-hyperintensity are not reliable diagnostic features of AVN as they can represent either oedema or immature fibrosis (7). Dynamic contrast-enhanced (DCE)-MRI is very useful for quantifying bone perfusion (8,9). The perfusion dynamics, however, of Kienbock's disease are different from those of established scaphoid or femoral head AVN (7). In the early stages of Kienbock's disease, when radiographs and CT are normal, and MRI shows diffuse lunate marrow oedema, relative lunate hyperperfusion may be seen, presumably due to increased capillary permeability secondary to ischaemia. Later in the disease, when a coronal fracture has occurred, hyper-perfusion in and around the fracture site occurs due to immature granulation tissue filling the fracture area as well as osmotic diffusion of contrast into the surrounding bone (10). DCE-MRI should be performed in the sagittal plane when a coronal fracture is present rather than the more usual coronal plane (9).

The main differential diagnosis of early Kienbock's disease on MR imaging is ulnocarpal impaction. Ulnocarpal impaction tends to (I) occur in rachet or other sports that involve gripping the handle with the wrist in ulnar deviation; (II) be associated with positive ulnar variance; (III) show bone marrow oedema most intense at the ulnar-proximal aspect of the lunate; (IV) have concomitant injury to the proximal lunate articular cartilage and articular disc of the triangular fibrocarilage complex (TFCC) as well as tear of the central membranous component of the luno-triquetral ligament; and (V) is not associated with lunate collapse, fragmentation, or fracture (6).

Carpal boss (Figure 2)

Carpal boss, also referred to as carpometacarpal (CMC) bossing or osseous protuberance, manifests as a bony protuberance on the dorsal aspect of the 2nd or 3rd metacarpal bone bases. This relatively uncommon condition typically presents between 20 and 40 years old. Patients with carpal bossing are often asymptomatic, though some, particularly athletes engaged in wrist extension activities such as gymnastics, golf, and racquet sports, develop symptoms such as dull pain, point tenderness, limited wrist extension, and moderate swelling or bony bump on the dorsum of the carpus (11). Symptoms may arise due to acute injury, ganglion cyst formation, or repetitive microtrauma leading to inflammation of an adventitial bursa between the extensor tendons and the bony prominence (12). Lateral radiography can usually reveal the dorsal bony prominence or irregularity at the metacarpal bone base. However, the bony prominence might be obscured by overlapping bones. A "carpal boss view" with the hand 30 degrees supinated and the ulnar deviated is helpful, although CT imaging is the preferred method of delineating carpal boss anatomy with reformatted views. MRI helps assess surrounding inflammation, osteoarthritis, and ganglion cyst formation (13). The carpal boss usually does not require surgical treatment unless significant symptoms persist despite splinting, activity modification, analgesia, and anti-inflammatory medication.

Figure 2 A 22-year-old male patient with dorsal wrist pain for one year. (A) Lateral wrist radiograph shows an additional osseous body articulating with the base of the 3rd metacarpal base, suggestive of a "carpal boss" at the 3rd CMC joint (solid arrow). (B) Sagittal proton-density fat suppression MR image of the same region shows a carpal boss articulating with the posterior aspect base 3rd metacarpal bone (block arrow). Premature osteoarthritis with mild marrow oedema and a tiny subchondral cyst (arrowhead) is present. CMC, carpometacarpal; MR, magnetic resonance.

Triquetral fracture (Figure 3)

Triquetral fracture is the second most common carpal fracture after scaphoid fracture, accounting for about 20% of carpal bone fractures (14). Most triquetral fractures occur due to a fall on the outstretched hand with ulnar deviation (14). There are three types of triquetral fracture: cortical dorsal, body, and palmar fracture. Dorsal cortical fractures are the most common (14). Typically, patients experience pain, swelling, and point tenderness on the dorsal and dorso-ulnar aspect of the wrist.

Triquetral fractures mainly occur in young to middle-aged individuals engaged in high-impact sports or following a high-impact fall onto the outstretched hand. Individuals with a long (>6 mm) ulnar styloid process and positive or neutral ulnar variance are more susceptible to triquetral fracture (15). This may be due to a chisel action of the ulnar styloid onto the dorsal cortical surface of the triquetrum. Avulsion of the extrinsic ligaments can also lead to a dorsal cortical fracture (16).

Radiography has only moderate sensitivity in detecting carpal bone fractures (17). About 20% of carpal bone fractures and 40% of triquetral fractures are radiographically occult due to their small size and obscuration by overlapping bone structures (18). CT is the gold standard to confirm or exclude carpal bone fracture if radiographs are negative (Welling). MR has the advantage of revealing bone marrow oedema indicative of trabecular microfracture, though it may not detect the small cortical fracture as clearly as CT. Avulsion fractures on the dorsal aspect of the triquetrum are often associated with visible ligamentous injury (19,20). Confirmation of ligament injury is, however, not an indication to undertake MRI if the fracture is adequately seen on radiographs or CT as it does not affect management. Most triquetral fractures are non-displaced or minimally displaced and can be treated effectively with immobilisation in a splint or cast.

Joints

Osteoarthritis (Figure 4)

Osteoarthritis centrally in the wrist is frequent occurrence in patients aged 75 years or older due to age-related cartilage thinning. Moderate to severe osteoarthritis in the central wrist area usually results from intrinsic wrist injuries such as

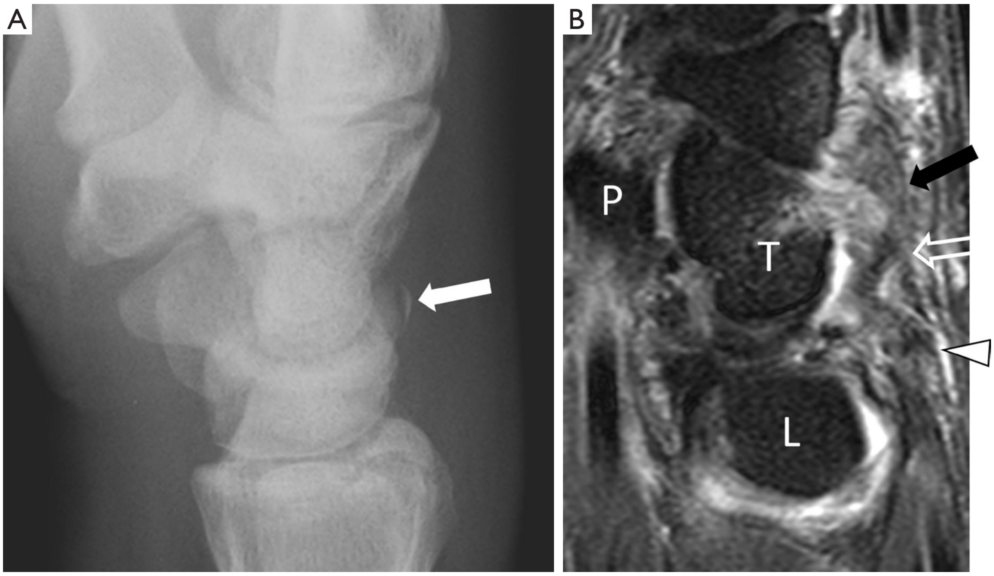

Figure 3 A 35-year-old male with severe dorsal wrist pain after fall during a football match. (A) Lateral wrist radiograph shows a small sharply demarcated osseous body (arrow) on the dorsal aspect of the carpus indicative of an acute triquetral fracture. (B) Sagittal T2-weighted fat suppressed MR of the same wrist shows how the low signal intensity cortical fracture fragment (block arrow) is barely visible. Associated severe sprain of dorsal intercarpal (black arrow) and radiocarpal (arrowhead) ligaments is seen with severe oedema and thickening of these ligaments. P, pisiform; T, triquetrum; L, lunate; MR, magnetic resonance.

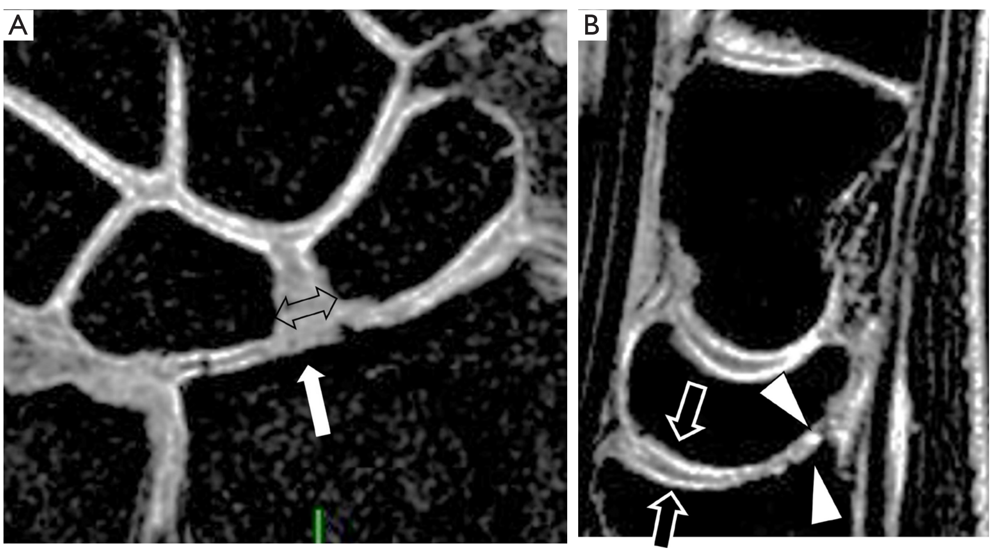

Figure 4 A 41-year-old male patient with intermittent dorsal wrist pain for 8 months following a wrist sprain two years earlier. (A) Coronal T2-fat suppressed gradient echo MR image showing moderate widening of the scapholunate interval (double arrow), suggestive of scapholunate ligament tear. Secondary osteoarthritis with moderate cartilage thinning radial aspect of lunate fossa (arrow) distal radius. (B) Sagittal gradient echo MR image showing cartilage thinning (arrowheads) on the dorsal aspect of the lunate fossa. The cartilage thickness on the ventral aspect of the lunate fossa is normal (block arrows). MR, magnetic resonance.

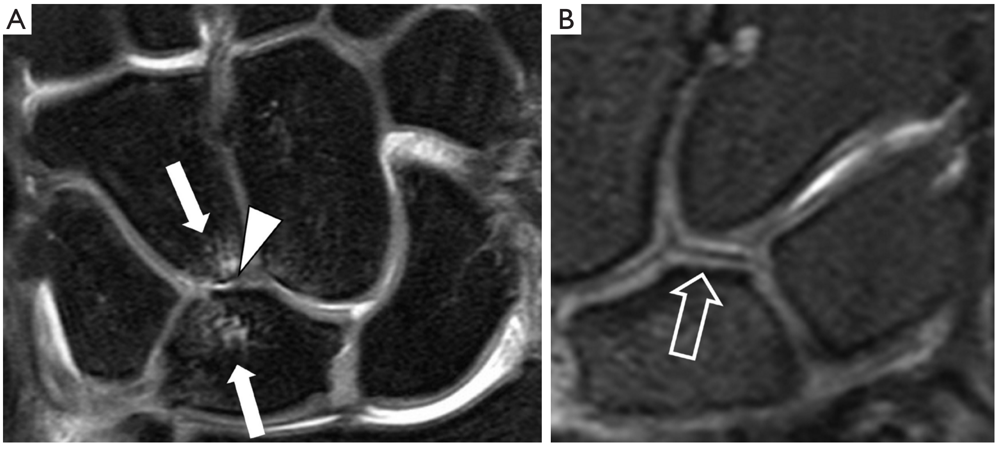

Figure 5 A 55-year-old female with dorsal wrist pain for one year and no history of trauma. (A) Coronal proton density fat-suppressed MR image of right wrist shows a type 2 lunate with an additional facet for articulation with the hamate. Moderate subarticular bone marrow oedema (solid arrows) is present of the hamatolunate joint with complete loss of articular cartilage focally (arrowhead). Features are compatible with hamatolunate impaction syndrome with severe osteoarthritis. (B) Normal subject with type 2 lunate (block arrow) and no hamatolunate impaction for comparison. MR, magnetic resonance.

carpal instability, scaphoid fracture, TFCC injury, or calcium pyrophosphate deposition disease (CPPD).

At the first CMC joint level, osteoarthritis usually affects the mobile first CMC joint rather than the much less mobile 2nd and 3rd CMC joints. Osteoarthritis of the 2nd and 3rd CMC joints usually follows traumatic capsuloligamentous injury (21). Patients typically present with localised dorsal wrist pain ± crepitus or painful laxity on stressing the CMC joints. Radiographs reveal characteristic osteoarthritic features with joint space narrowing, marginal osteophytes and, in more advanced diseases, subchondral sclerosis and cysts. Radiographs alone will usually suffice, though CT will provide a more detailed assessment if surgical ankylosis is being considered. MRI is usually not necessary to evaluate wrist osteoarthritis.

Standard MRI is limited in evaluating osteoarthritis of the radiocarpal, intercarpal, and CMC joints where the articular cartilage is thin (22-25). Compared to cadaveric specimens, 3T MRI had a sensitivity of only 50% for detecting wrist joint cartilage loss (26). Specialised three-dimensional cartilage sequences offer improved resolution. MR arthrography, with or without wrist traction, enhances the visibility of wrist articular cartilage compared to standard MR (27,28).

Hamatolunate impaction (Figure 5)

Hamatolunate impaction is due to repetitive compression between the proximal apex of the hamate and the lunate. The impaction occurs in patients with a Type II lunate, i.e., a lunate with an additional facet articulating with the hamate bone, which can be seen on radiographs (29). Hamatolunate impaction commonly affects athletes engaged in sports stressing the wrist joint, such as racquet or gymnastics. Typical symptoms are central to ulnar-paracentral dorsal wrist pain, as well as restricted flexion and extension. Repetitive hamatolunate impaction predisposes to focal chondromalacia, cartilage loss, subchondral bone marrow oedema, subcortical cysts, and synovitis at the proximal aspect of the lunate, all of which can be seen on MR imaging (8). Treatment is rest, immobilisation, anti-inflammatory medication, and physical therapy. When conservative management fails, arthroscopic burring of the hamate apex may be helpful.

Inflammatory joint disease (Figures 6-8)

The wrist is the most affected joint in rheumatoid arthritis (RA), with inflammation in the wrist being a useful marker of systemic disease. Pain, stiffness, and swelling on the dorsal aspect of the wrist are typical presenting features.

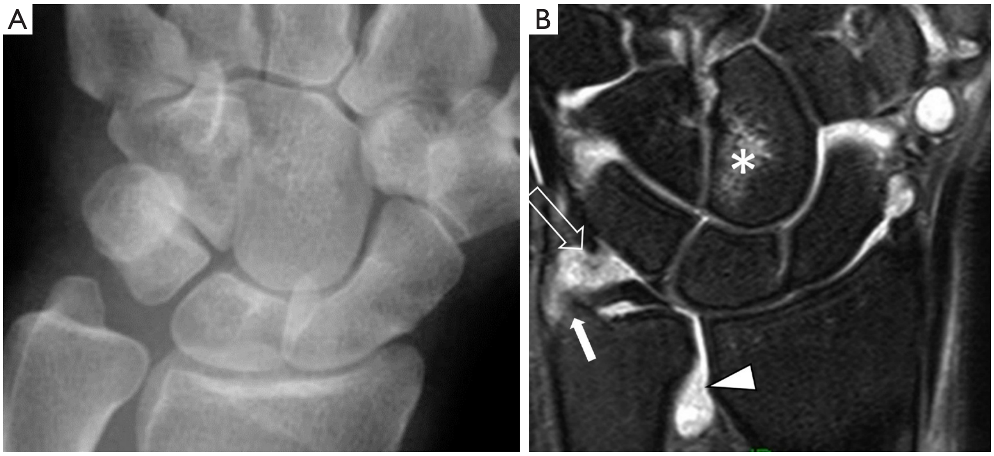

Figure 6 A 47-year-old female with unilateral right wrist pain for ten months, predominantly on the dorsal aspect of the wrist. (A) Frontal radiograph of the wrist is normal. (B) Coronal T2-weighted fat suppressed MR image shows moderate synovial proliferation in the pre-styloid recess (block arrow) and distal radio-ulnar joint (arrowhead). Subtle erosion of the ulnar styloid process (solid arrow) is present with mild bone marrow oedema of the capitate (asterisk). Features are indicative of early rheumatoid arthritis. MR, magnetic resonance.

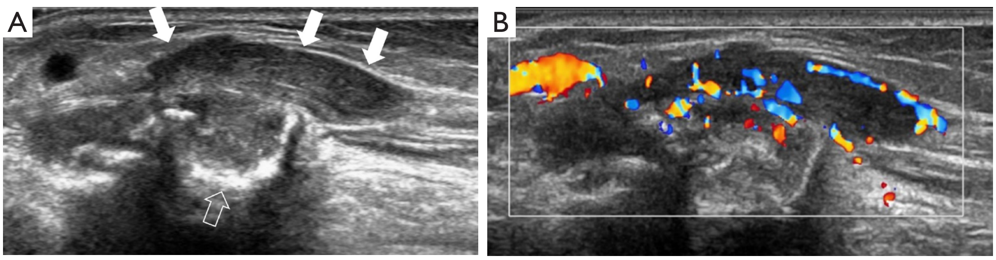

Figure 7 Another 56-year-old female patient with more severe pain and swelling for more than half a year. (A) Longitudinal ultrasound of wrist shows severe synovial proliferation (solid arrows) on the dorsal aspect of the ulnar head with a medium-sized underlying erosion (block arrow). (B) Colour Doppler ultrasound shows severe synovial hyperaemia indicative of active disease.

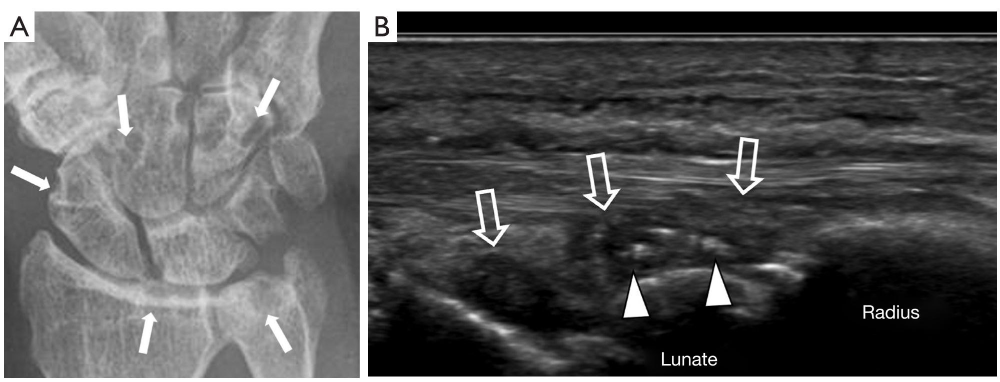

Figure 8 A 57-year-old male patient with dorsal wrist pain for one year. (A) Frontal radiograph shows multiple well-defined erosions in the carpal bones, distal ulna and radius (solid arrows) indicative of an erosive arthropathy. (B) Longitudinal ultrasound shows mild synovial proliferation (block arrows) containing small echogenic foci (arrowheads), suggestive of crystal aggregates. Overall features are highly suspicious of a crystal arthropathy, more likely due to gout rather than CPPD. CPPD, calcium pyrophosphate deposition disease.

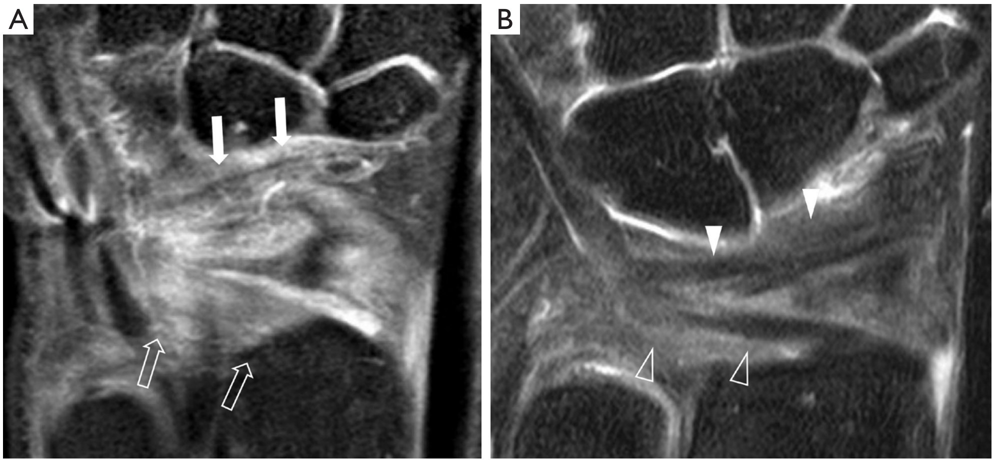

Figure 9 A 35-year-old female patient presented with acute dorsal wrist pain after slipped and fell. (A) Coronal T2-weighted fat suppression MR image shows severe thickening and oedema of the dorsal intercarpal (arrows) and dorsal radiocarpal ligaments (block arrows) suggestive of sprain ligament. The ligament is still in continuity. (B) Normal appearance of the dorsal ligaments on the same sequence of another subject was used for comparison. Dorsal intercarpal (arrowheads) and dorsal radiocarpal ligament (block arrowheads) show low T2-weighted signal intensity with smaller in calibre. MR, magnetic resonance.

Less common causes of inflammatory wrist arthritis include crystal arthritis [due to gout or crystal pyrophosphate deposition (CPPD) disease] and psoriatic arthritis.

Increased awareness and understanding have enabled RA to be diagnosed at an earlier stage. Early RA is defined as symptom duration of less than two years. Early RA is more responsive to treatment than chronic RA. Radiographs will usually be normal in early RA. A small percentage of patients will have radiographically visible erosions, while none will have detectable joint space narrowing (30).

Ultrasound is often more sensitive and specific than clinical examination or radiography identifying synovitis and erosions. Colour Doppler ultrasound, especially with 'superb microvascular imaging' or analogous vascular enhancement techniques, enables the assessment of synovial hyperaemia as a feature of synovial activity (31); additionally, ultrasound aids in identifying tenosynovitis, a common accompaniment of early RA.

CT imaging does not usually form part of the routine imaging workup in patients with suspected RA, though it can detect subtle radiographically occult erosions. CT is also highly sensitive in detecting calcium deposits in CPPD, while dual-energy CT will reveal monosodium urate crystals in tophaceous gout. MRI also does not currently form part of the routine workup of RA patients. However, it is very accurate at revealing and quantifying synovitis, tenosynovitis, and osteitis, as well as erosions and joint space narrowing. In patients presenting with early RA, almost 20% will have wrist synovitis only, nearly 80% will have both synovitis and tenosynovitis, while about 2% will have tenosynovitis with minimal or no synovitis (30).

Mild reactive-type synovial proliferation is very commonly seen following wrist trauma, with ganglion leakage or with wrist osteoarthritis and milder forms of inflammatory arthritis. Moderate to severe synovial hypertrophy is a feature of inflammatory arthritis, includes TB infection, or synovial tumour such as pigmented villonodular synovitis (PVNS) and synovial (osteo)chondromatosis. Ultrasound-guided synovial biopsy is very helpful to exclude or confirm infection or synovial tumours (32,33).

Ligaments

Extrinsic ligament tear (Figure 9)

The main dorsal carpal ligaments (radiocarpal, and ulnotriquetral) insert onto the dorsum of the triquetrum (8). Dorsal extrinsic ligament injuries may result in dorsal wrist pain and, much less frequently, SL or mid-carpal instability.

The MR features of a ligament sprain are ligamentous and peri-ligamentous swelling and oedema; partial fibre discontinuity is a feature of partial ligament tears, while complete fibre discontinuity indicates complete ligament tears (34). Most (~85%) extrinsic ligament tears are sprains (grade 1), with a small percentage (~10%) being

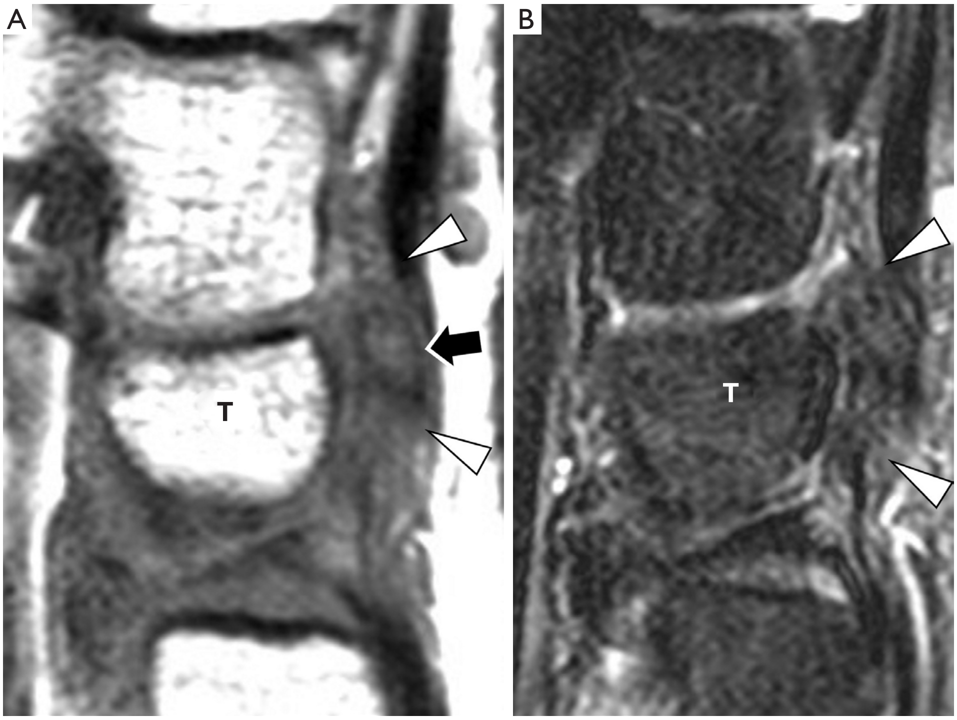

Figure 10 A 41-year-old patient slipped and fell 4 months ago with diagnosis of triquetral fracture. He suffered from persistent dorsal wrist pain and swelling. (A) Sagittal T1-weighted and (B) T2-weighted fat suppression MRI images of the same patient show a small osseous body with rim of hypointense T1- and T2-weight signal suggestive of well corticated margin at dorsal side of the T, suggestive of a non-united fracture (arrow). There is associated soft tissue thickenings with low T1W (arrowheads) and low T2W signal intensity at around the fracture which suggests hypertrophic scars. T, triquetrum; MRI, magnetic resonance imaging; T2W, T2-weighted; T1W, T1-weighted.

partial tears (grade 2). Full-thickness tears (grade 3) are uncommon (<5%) (19).

The interaction of intrinsic and extrinsic ligaments to stabilize the wrist and carpus is complex. Arthroscopy plays an important role in diagnosis and staging. Arthroscopy is the gold standard to confirm and consolidate the diagnosis of the underlying cause for carpal instability including the carpal instability nondissociative (CIND) or carpal instability dissociative (CID) disease. Arthroscopic repair of extrinsic ligament tears is feasible (35). Ultrasound can visualize most extrinsic ligaments, although MRI evaluation is better (36), enabling the visualization of individual extrinsic ligaments and assessment of carpal alignment as a feature of carpal instability (37).

Dorsal wrist capsular impingement (DWCI) (Figures 10,11)

DWCI is caused by inflammation and impingement of the redundant dorsal wrist capsule/synovium between the dorsal ridge of the scaphoid and the extensor carpi radialis brevis (ECRB) tendon. This may occur from acute trauma, chronic repetitive microtrauma, or osteoarthritis. Patients experience swelling and pain localized to the dorsal and central wrist area during passive wrist extension (38). While DWCI is primarily a clinical diagnosis, CT can reveal the presence of small contributory osteophytes (39). MRI helps exclude other causes of dorsal wrist pain and can reveal the dorsal capsular thickening, ± synovitis and soft tissue inflammation indicative of DDWCI (39). Treatment includes rest, activity modification, anti-inflammatory medication, physical therapy, and occasionally corticosteroid injections. Severe or persistent cases may benefit from surgical intervention (38).

SL ligament tear (dorsal side) with ganglion cyst (Figures 12,13)

The SL ligament is the most important wrist ligament.

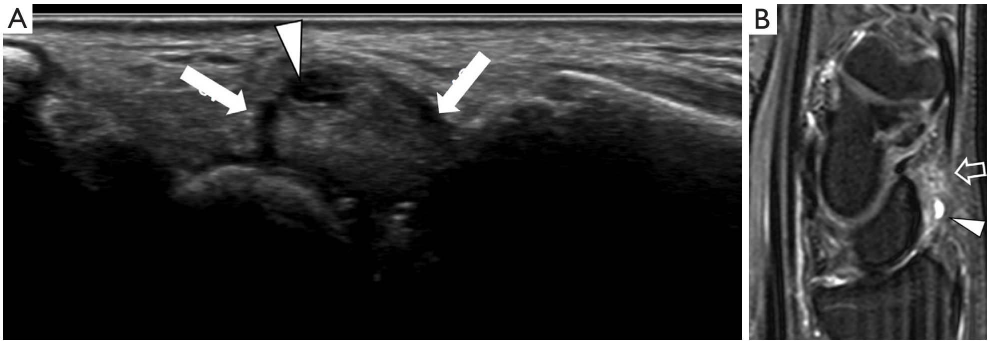

Figure 11 A 51-year-old female with dorsal wrist pain for half a year and a clinically vague thickening of the capitolunate joint area. (A) Longitudinal ultrasound shows focal nodular thickening of the radiolunate interval (arrows) associated with a small ganglion cyst (arrowhead) suggestive of chronic sprain ligament. (B) Sagittal T2-weighted fat suppressed MR image confirms focal ligament thickening and oedema of the dorsal radiocarpal ligament (block arrow) and a small ganglion cyst (arrowhead). MR, magnetic resonance.

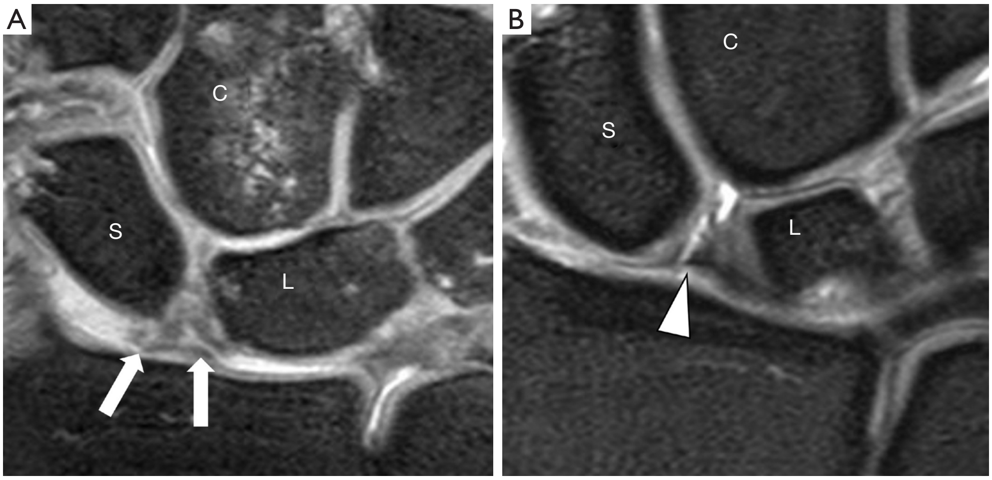

Figure 12 Two male patients presented with dorsal wrist pain after wrist injury. (A) Coronal proton-density fat suppressed MR image shows severe swelling and disruption of the SL ligament indicative of tear with scar formation (arrows). (B) Coronal proton-density fat suppressed MRI image of another patient shows slit-like full-thickness tear of the membranous component of the SL ligament (arrowhead). C, capitate; S, scaphoid; L, lunate; MR, magnetic resonance; SL, scapholunate; MRI, magnetic resonance imaging.

It stabilizes the central aspect of the proximal carpal row, where forces are transmitted from the hand to the distal forearm. It is a frequently torn ligament which may lead to SL instability (40). Acute SL ligament tear may occur in conjunction with scaphoid or distal radial fracture (41,42). The saddle-shaped SL and lunotriquetral (LT) ligaments have three components, with the fibrous dorsal and volar components of the SL ligament being stronger and more functionally important than the central fibrocartilaginous membranous component (43,44). The LT ligament is less frequently torn than the SL ligament.

Radiography cannot directly visualize the SL ligament, though SL dissociation with widening (>4 mm) of the SL interspace can be seen on radiographs. SL widening may occur in the absence of SL tear or dissociation. LT ligament tear is not commonly associated with the widening of the LT interval until the later stages (45).

Lateral radiographs may reveal an increase in the SL (>60 degrees) or capitolunate (CL) (>30 degrees) angles indicating mid-carpal instability (8). Severe SL tear leads to dorsal intercalated segmental instability (DISI) with dorsal angulation of the lunate. Severe LT tear leads to

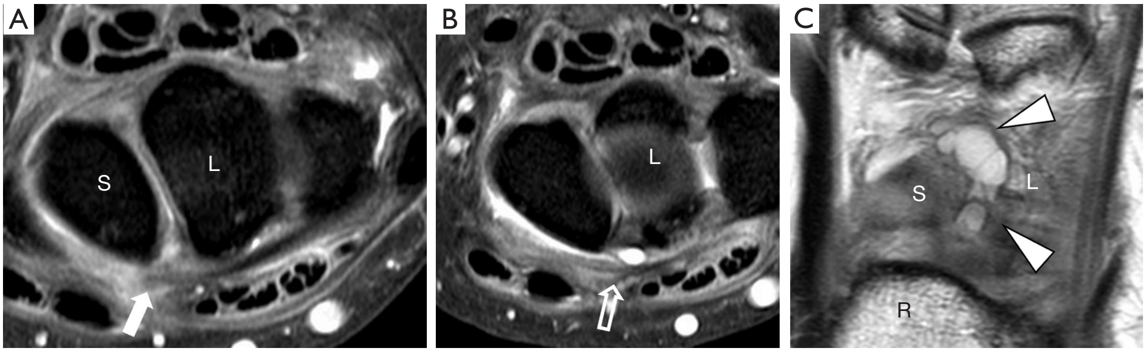

Figure 13 A 38-year-old patient with dorsal wrist pain and swelling for one year after a wrist sprain. (A) Axial proton-density fat suppressed MR image showing a full-thickness tear of the dorsal component SL ligament (arrow). (B) More distally, there is a small ganglion cyst extending through this tear (block arrow). (C) Coronal proton-density image dorsum of wrist shows the multiloculated ganglion cyst (arrowheads). S, scaphoid; L, lunate; R, radius; MR, magnetic resonance; SL, scapholunate.

volar intercalated segmental instability (VISI) with volar angulation of the lunate. Either DISI or VISI deformity can result in proximal migration of the distal carpal row, leading to scapholunate advanced collapse (SLAC).

SLAC is categorized into four stages: stage I—radioscaphoid osteoarthritis distally; stage II—diffuse radioscaphoid osteoarthritis; stage III—mid-carpal osteoarthritis; stage IV—radiolunate osteoarthritis (44,46). Radiographically, the scaphoid appears foreshortened and slightly pronated, creating a scaphoid "ring" configuration (47). Ultrasound can visualise the dorsal and, to a lesser degree, the volar fibres of the SL and LT ligaments (36,48). MRI is the best imaging modality to evaluate the intrinsic ligaments though the gold standard for diagnosis is still wrist arthroscopy. The dorsal and volar components are best evaluated on axial images (49). Because of its obliquity, the LT ligament is more difficult to see than the SL ligament. Oblique axial imaging oriented parallel to the individual ligament is helpful in delineating the volar and dorsal LT components more clearly (50,51). Coronal imaging is used to visualize the central membranous portion of the SL and LT ligaments (50). MRI features of a complete tear include the absence of the ligament and full-thickness ligament discontinuity. Partial tears are seen as either partial thickness ligament discontinuity, ligament swelling, fraying, or thinning (52). Age-related perforations of the membranous portions of both the LT and SL ligaments are common in asymptomatic subjects (53).

MR arthrography ± traction can increase the accuracy of MRI in detecting intrinsic ligament tears. MR arthrography has a higher sensitivity (89%) and accuracy (98%) than non-arthrography MRI [sensitivity (50%), accuracy (60%)] for detecting tears of the membranous component of the SL ligament (54). Arthrography with traction increases central tear detection accuracy to almost 100% (27).

Dorsal capsulo-scapholunate septum (DCSS) (Figure 14)

The DCSS is positioned between the dorsal component of the SL interosseous ligament and the dorsal intercarpal ligament (55). It acts as a secondary for the SL joint (55). However, DCSS often cannot be reliably assessed with MRI and the gold standard is wrist arthroscopy. Isolated tear of the DCSS may manifest as a ganglion cyst. Ganglion cysts arising from DCSS will not communicate with the SL joint. Isolated tears of the DCSS can be associated with SL instability in the absence of an injury to the SL ligament.

Tendons

Tendinosis

Tendinosis is associated with increased proteoglycan deposition with the tendon substance, leading to tendon thickening, fibrillary disruption, and propensity to tears. The extensor digitorum communis, extensor pollicis longus, and extensor digiti minimi are frequently affected on the dorsum of the wrist. Tendinosis per se is typically asymptomatic, though it can be associated with varying degrees of peritendinitis, which can lead to dorsal wrist pain. Evaluation is best performed with ultrasound or MRI. Tendinosis can also lead to spontaneous tendon tears, particularly of the extensor pollicis longus tendon, as it

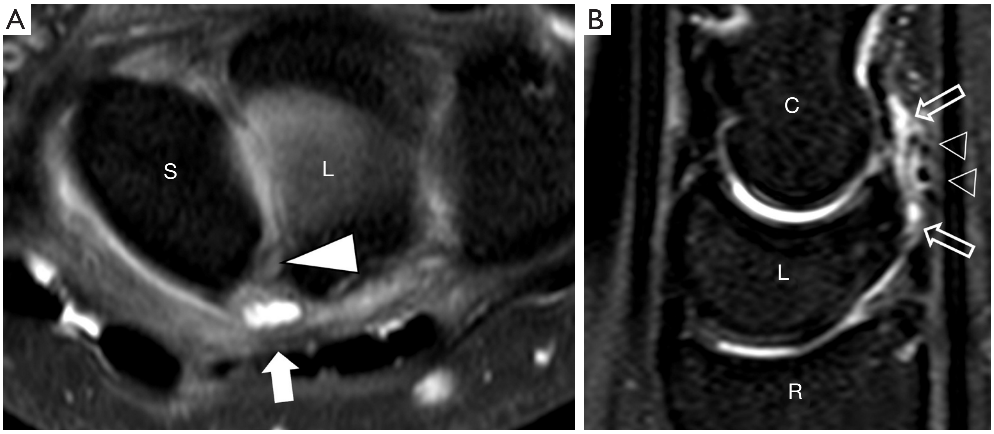

Figure 14 A 35-year-old patient with dorsal wrist pain and swelling for one month. (A) Axial proton-density fat suppressed MR image shows a small ganglion cyst located between the dorsal component scapholunate ligament (solid arrowhead) and dorsal radiocarpal ligament (solid arrow). The dorsal component of the scapholunate ligament is normal. (B) Sagittal T2-weighted fat suppressed image shows fluid (block arrows) deep to the dorsal radiocarpal ligament (block arrowheads), suggestive of dorsal capsular septum tear. S, scaphoid; L, lunate; R, radius; C, capitate; MR, magnetic resonance.

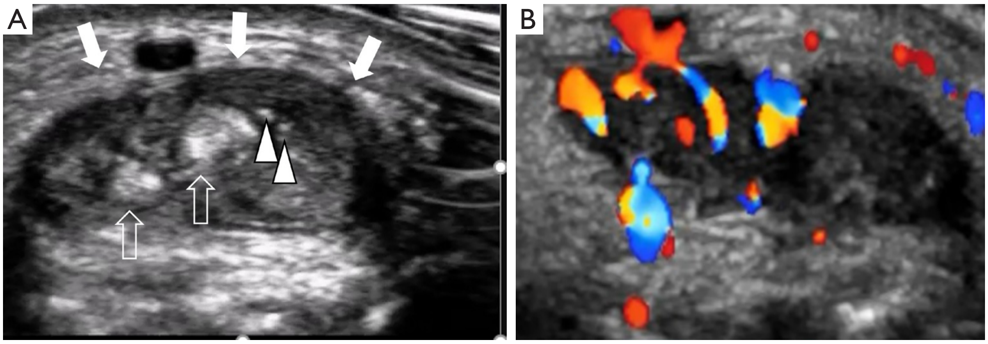

Figure 15 A 68-year-old male patient with dorsal wrist redness and swelling and restriction of finger extension. (A) Transverse ultrasound shows severe tenosynovial thickening (arrows) of EDC with moderate tendon thickening (block arrows). There are multiple small echogenic foci (arrowheads) within both the thickened tenosynovium and the thickened extensor tendons, indicative of gouty tenosynovitis. (B) Colour Doppler ultrasound shows severe tenosynovial hyperaemia indicative of active inflammation. EDC, extensor digitorum communis.

angles around Lister's tubercle on the dorsum of the distal radius.

Tenosynovitis (Figures 15,16)

All wrist tendons, except for the flexor carpi ulnaris and palmaris longus, have a tendon sheath or tendon sheath equivalent. The extensor digitorum communis is most commonly affected by tenosynovitis in early RA, gout and chronic infections such as tuberculosis. Depending on chronicity, ultrasound will reveal tenosynovial effusion or tenosynovial proliferation. Inflammatory arthritis, gout, and infection produce more severe tenosynovitis than repetitive injury (56). Numerous echogenic foci, representing crystal aggregates within the thickened tenosynovium is a feature of gouty tenosynovitis.

Mass

Ganglion cyst (Figures 17,18)

Ganglion cysts constitute about 70% of all soft tissue masses in the hand and wrist region (57). Symptomatic ganglia are most common on the dorsal aspect of the wrist (58). On

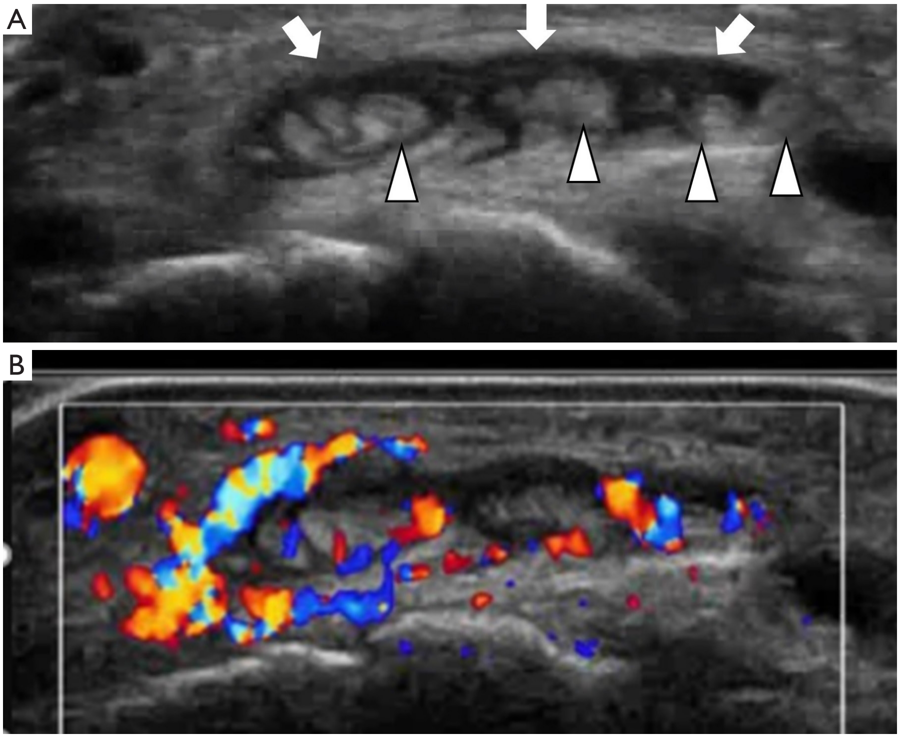

Figure 16 A 46-year-old female patient with dog bite several weeks previously followed by slowly progressive swelling dorsum of wrist. (A) Transverse ultrasound shows moderate tenosynovial thickening (arrows) of EDC. The extensor digitorum tendons (arrowheads) are mildly swollen and surrounded by moderately thickened tenosynovium. (B) Colour Doppler ultrasound shows severe tenosynovial hyperaemia indicative of active inflammation. In this clinical context, features are suggestive of infective tenosynovitis (microbiology confirmed). EDC, extensor digitorum communis.

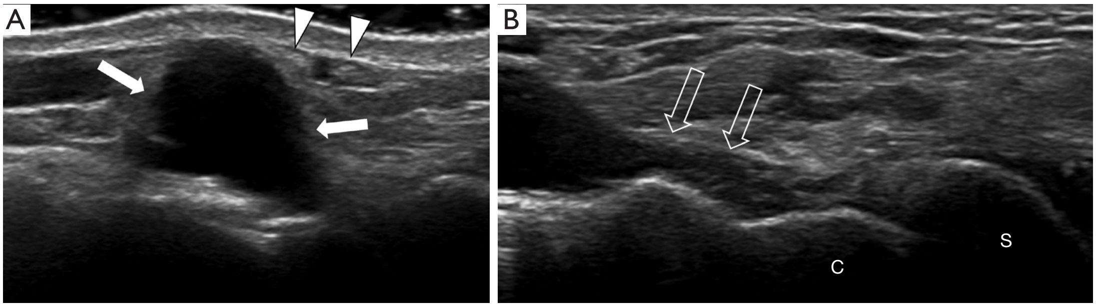

Figure 17 A 58-year-old female patient with dorsal wrist pain and swelling. (A) Transverse ultrasound shows well-defined anechoic cyst (solid arrows) present under the clinically palpable swelling deep to the EDC (arrowheads), indicative of a ganglion cyst. (B) Longitudinal ultrasound of the same area shows a tract extending from the ganglion to the scaphocapitate articulation (block arrows) indicative of a ganglion cyst arising from the dorsal aspect of this joint. C, capitate; S, scaphoid; EDC, extensor digitorum communis.

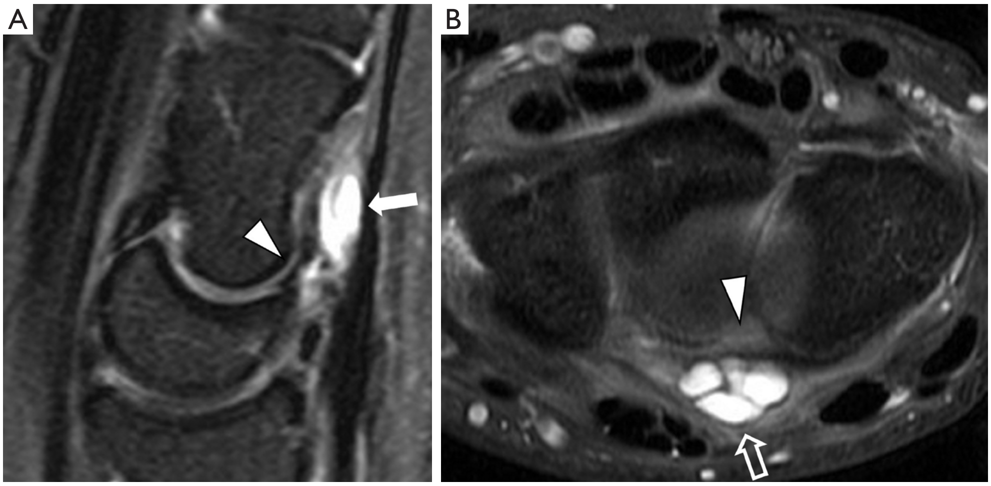

Figure 18 A 49-year-old male patient with dorsal wrist pain for a few months and no clinical swelling. (A) Sagittal T2W fat-suppressed MR image showing a small multiloculated cystic lesion (solid arrow) on the dorsal aspect of the mid-carpus deep to the extensor digitorum communis and superficial to the dorsal component of the SL ligament (arrowhead). Features are indicative of an occult ganglion. (B) Axial T2W fat-suppressed MR image shows the ganglion (block arrow) lying superficial to the intact SL ligament (arrowhead). No tear was seen. This is suggestive of a cyst arising from the DCSS. T2W, T2-weighted; MR, magnetic resonance; SL, scapholunate; DCSS, dorsal capsulo-scapholunate septum.

the dorsal surface, ganglia arise most commonly from the SL joint ligament due to high tensile forces and mechanical impingement of the SL ligament during extended wrist weight-bearing positions, leading to degeneration and mechanical trauma (2,59,60).

Ganglia will extend from the joint through the dorsal SL intrinsic ligament, through or between the extrinsic ligaments and into the subcutaneous tissues. Pain may be due to the recent emergence of a ganglion ± leakage of ganglion contents ± compression of the terminal portion of the posterior interosseous nerve (58). Clinically, point tenderness over the SL interval during wrist hyperextension, ± a localised swelling or mass are typical (61). Ultrasound is very accurate at identifying ganglion cysts ± guiding aspiration ± hyaluronidase injection. MRI is more sensitive to detecting peri-ganglionic soft tissue inflammation following recent leakage of ganglionic content (6). MRI is also more helpful in precisely determining the deep communication between the ganglion cyst and the joint, which is helpful as this deep tract needs to be excised, if surgery is undertaken, to prevent recurrence.

Soft tissue masses (Figure 19)

Localised swelling, rather than pain, is usually the dominant presenting feature for masses arising on the dorsum of the wrist, such as giant cell tumour of tendon sheath (GCTTS) or nerve sheath tumour rather than pain (62,63). Most have fairly typical ultrasound and MRI appearances, enabling the diagnosis to be suggested and usually confirmed by percutaneous biopsy before definitive surgical excision (64).

Conclusions

Pain on the dorsal side of the wrist is a common clinical presentation and the dorsal wrist region has distinct anatomical features with a wide spectrum of pathologies. The role of imaging, particularly MRI in diagnosing dorsal wrist pain is expected to expand further in the future. This review has discussed the imaging characteristics of both common and uncommon pathologies in details. This comprehensive approach underscores the critical role of advanced imaging in contemporary clinical practice.

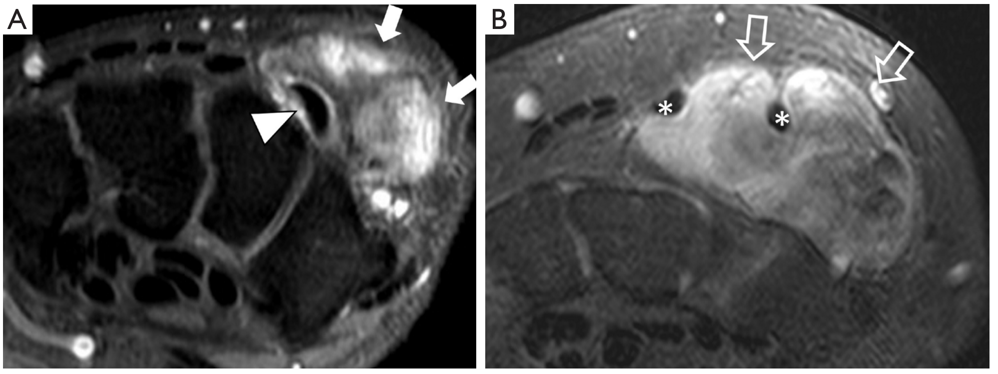

Figure 19 Two male patients with dorsal wrist pain and swelling. (A) Axial T2W fat suppressed MR image shows a solid partially hyperintense mass (solid arrows) encasing the ECRB (arrowhead). GCTTS is the most likely consideration, which was confirmed histologically. (B) Axial T2W fat suppressed MR image of another patient shows a similar mass (block arrows) encasing the ECRB and the index finger extensor digitorum tendons (*). Although the MR appearances were suggestive of GCTTS, the histological diagnosis was sarcoma. T2W, T2-weighted; MR, magnetic resonance; ECRB, extensor carpi radialis brevis; GCTTS, giant cell tumour of tendon sheath.

Acknowledgments

Funding: None.

Footnote

Conflicts of Interest: All authors have completed the ICMJE uniform disclosure form (available at https://qims.amegroups.com/article/view/10.21037/qims-24-420/coif). J.F.G. serves as an unpaid editorial board member of *Quantitative Imaging in Medicine and Surgery*. The other authors have no conflicts of interest to declare.

Ethical Statement: The authors are accountable for all aspects of the work in ensuring that questions related to the accuracy or integrity of any part of the work are appropriately investigated and resolved.

References

1. Webb BG, Rettig LA. Gymnastic wrist injuries. Curr Sports Med Rep 2008;7:289-95.
2. Nance EM, Byun DJ, Endo Y, Wolfe SW, Lee SK. Dorsal Wrist Pain in the Extended Wrist-Loading Position: An MRI Study. J Wrist Surg 2017;6:276-9.
3. Szabo RM. Distal radioulnar joint instability. J Bone Joint Surg Am 2006;88:884-94.
4. Bonzar M, Firrell JC, Hainer M, Mah ET, McCabe SJ. Kienböck disease and negative ulnar variance. J Bone Joint Surg Am 1998;80:1154-7.
5. Lutsky K, Beredjiklian PK. Kienböck disease. J Hand Surg Am 2012;37:1942-52.
6. Watanabe A, Souza F, Vezeridis PS, Blazar P, Yoshioka H. Ulnar-sided wrist pain. II. Clinical imaging and treatment. Skeletal Radiol 2010;39:837-57.
7. Ng AW, Griffith JF, Taljanovic MS, Li A, Tse WL, Ho PC. Is dynamic contrast-enhanced MRI useful for assessing proximal fragment vascularity in scaphoid fracture delayed and non-union? Skeletal Radiol 2013;42:983-92.
8. Cerezal L, del Piñal F, Abascal F, García-Valtuille R, Pereda T, Canga A. Imaging findings in ulnar-sided wrist impaction syndromes. Radiographics 2002;22:105-21.
9. Griffith JF, Yip SWY, van der Heijden RA, Valenzuela RF, Yeung DKW. Perfusion Imaging of the Musculoskeletal System. Magn Reson Imaging Clin N

Am 2024;32:181-206.
10. Anderson SE, Steinbach LS, Tschering-Vogel D, Martin M, Nagy L. MR imaging of avascular scaphoid nonunion before and after vascularized bone grafting. Skeletal Radiol 2005;34:314-20.
11. Park MJ, Namdari S, Weiss AP. The carpal boss: review of diagnosis and treatment. J Hand Surg Am 2008;33:446-9.
12. Conway WF, Destouet JM, Gilula LA, Bellinghausen HW, Weeks PM. The carpal boss: an overview of radiographic evaluation. Radiology 1985;156:29-31.
13. Poh F. Carpal boss in chronic wrist pain and its association with partial osseous coalition and osteoarthritis - A case report with focus on MRI findings. Indian J Radiol Imaging 2015;25:276-9.
14. Hey HW, Chong AK, Murphy D. Prevalence of carpal fracture in Singapore. J Hand Surg Am 2011;36:278-83.
15. Levy M, Fischel RE, Stern GM, Goldberg I. Chip fractures of the os triquetrum: the mechanism of injury. J Bone Joint Surg Br 1979;61-B:355-7.
16. Smith DK, Murray PM. Avulsion fractures of the volar aspect of triquetral bone of the wrist: a subtle sign of carpal ligament injury. AJR Am J Roentgenol 1996;166:609-14.
17. Jørgsholm P, Thomsen NO, Besjakov J, Abrahamsson SO, Björkman A. The benefit of magnetic resonance imaging for patients with posttraumatic radial wrist tenderness. J Hand Surg Am 2013;38:29-33.
18. Welling RD, Jacobson JA, Jamadar DA, Chong S, Caoili EM, Jebson PJ. MDCT and radiography of wrist fractures: radiographic sensitivity and fracture patterns. AJR Am J Roentgenol 2008;190:10-6.
19. Becce F, Theumann N, Bollmann C, Omoumi P, Richarme D, Guerini H, Campagna R, Meuli R, Drapé JL. Dorsal fractures of the triquetrum: MRI findings with an emphasis on dorsal carpal ligament injuries. AJR Am J Roentgenol 2013;200:608-17.
20. Guo RC, Cardenas JM, Wu CH. Triquetral Fractures Overview. Curr Rev Musculoskelet Med 2021;14:101-6.
21. Joseph RB, Linscheid RL, Dobyns JH, Bryan RS. Chronic sprains of the carpometacarpal joints. J Hand Surg Am 1981;6:172-80.
22. Nagy L. Salvage of post-traumatic arthritis following distal radius fracture. Hand Clin 2005;21:489-98.
23. Bordalo-Rodrigues M, Schweitzer M, Bergin D, Culp R, Barakat MS. Lunate chondromalacia: evaluation of routine MRI sequences. AJR Am J Roentgenol 2005;184:1464-9.
24. Haims AH, Moore AE, Schweitzer ME, Morrison WB, Deely D, Culp RW, Forman HP. MRI in the diagnosis of cartilage injury in the wrist. AJR Am J Roentgenol 2004;182:1267-70.
25. Mutimer J, Green J, Field J. Comparison of MRI and wrist arthroscopy for assessment of wrist cartilage. J Hand Surg Eur Vol 2008;33:380-2.
26. Saupe N, Prüssmann KP, Luechinger R, Bösiger P, Marincek B, Weishaupt D. MR imaging of the wrist: comparison between 1.5- and 3-T MR imaging--preliminary experience. Radiology 2005;234:256-64.
27. Lee RK, Griffith JF, Ng AW, Nung RC, Yeung DK. Wrist Traction During MR Arthrography Improves Detection of Triangular Fibrocartilage Complex and Intrinsic Ligament Tears and Visibility of Articular Cartilage. AJR Am J Roentgenol 2016;206:155-61.
28. Lee RK, Griffith JF, Tang WK, Ng AW, Yeung DK. Effect of traction on wrist joint space and cartilage visibility with and without MR arthrography. Br J Radiol 2017;90:20160932.
29. Malik AM, Schweitzer ME, Culp RW, Osterman LA, Manton G. MR imaging of the type II lunate bone: frequency, extent, and associated findings. AJR Am J Roentgenol 1999;173:335-8.
30. Xiao F, Griffith JF, Ko JKL, Yue J, Leung JCS, Yeung DKW, Tam LS. MRI wrist in early rheumatoid arthritis: reduction in inflammation assessed quantitatively during treatment period correlates best with clinical improvement. Skeletal Radiol 2021;50:1337-45.
31. Lopez-Ben RR. Assessing rheumatoid arthritis with ultrasound of the hands. AJR Am J Roentgenol 2011;197:W422.
32. Sitt JC, Griffith JF, Wong P. Ultrasound-guided synovial biopsy. Br J Radiol 2016;89:20150363.
33. Yip SWY, Griffith JF. Image-guided synovial biopsy with a focus on neoplastic lesions. Skeletal Radiol 2023;52:817-29.
34. Chhabra A, Soldatos T, Thawait GK, Del Grande F, Thakkar RS, Means KR Jr, Carrino JA. Current perspectives on the advantages of 3-T MR imaging of the wrist. Radiographics 2012;32:879-96.
35. Merlini L, Mathoulin C. Arthroscopic Repair of the Dorsal Intercarpal Ligament Detachment from the Scaphoid. J Wrist Surg 2021;10:539-42.
36. Taljanovic MS, Goldberg MR, Sheppard JE, Rogers LF. US of the intrinsic and extrinsic wrist ligaments and triangular fibrocartilage complex--normal anatomy and imaging technique. Radiographics 2011;31:e44.
37. Bateni CP, Bartolotta RJ, Richardson ML, Mulcahy H, Allan CH. Imaging key wrist ligaments: what the surgeon needs the radiologist to know. AJR Am J Roentgenol

2013;200:1089-95.
38. Matson AP, Dekker TJ, Lampley AJ, Richard MJ, Leversedge FJ, Ruch DS. Diagnosis and Arthroscopic Management of Dorsal Wrist Capsular Impingement. J Hand Surg Am 2017;42:e167-74.
39. Hanson ZC, Lourie GM. Middorsal Wrist Pain in the High-Level Athlete: Causes, Treatment, and Early Return to Play. Orthop J Sports Med 2022;10:23259671221088610.
40. Timins ME, Jahnke JP, Krah SF, Erickson SJ, Carrera GF. MR imaging of the major carpal stabilizing ligaments: normal anatomy and clinical examples. Radiographics 1995;15:575-87.
41. Neuhaus V, Jupiter JB. Current concepts review: carpal injuries - fractures, ligaments, dislocations. Acta Chir Orthop Traumatol Cech 2011;78:395-403.
42. Pollock J, Giachino AA, Rakhra K, DiPrimio G, Hrushowy H, Conway AF, Andreyechen M. SLAC wrist in the absence of recognised trauma and CPPD. Hand Surg 2010;15:193-201.
43. Peterson B, Szabo RM. Carpal osteoarthrosis. Hand Clin 2006;22:517-28; abstract vii.
44. Zlatkin MB, Rosner J. MR imaging of ligaments and triangular fibrocartilage complex of the wrist. Magn Reson Imaging Clin N Am 2004;12:301-31, vi-vii.
45. van Schoonhoven J, Prommersberger KJ, Schmitt R. Traumatic disruption of a fibrocartilage lunate-triquetral coalition--a case report and review of the literature. Hand Surg 2001;6:103-8.
46. Crema MD, Zentner J, Guermazi A, Jomaah N, Marra MD, Roemer FW. Scapholunate advanced collapse and scaphoid nonunion advanced collapse: MDCT arthrography features. AJR Am J Roentgenol 2012;199:W202-7.
47. De Filippo M, Sudberry JJ, Lombardo E, Corradi M, Pogliacom F, Ferrari FS, Bocchi C, Zompatori M. Pathogenesis and evolution of carpal instability: imaging and topography. Acta Biomed 2006;77:168-80.
48. Griffith JF, Chan DP, Ho PC, Zhao L, Hung LK, Metreweli C. Sonography of the normal scapholunate ligament and scapholunate joint space. J Clin Ultrasound 2001;29:223-9.
49. Lee RK, Ng AW, Tong CS, Griffith JF, Tse WL, Wong C, Ho PC. Intrinsic ligament and triangular fibrocartilage complex tears of the wrist: comparison of MDCT arthrography, conventional 3-T MRI, and MR arthrography. Skeletal Radiol 2013;42:1277-85.
50. Lee RK, Griffith JF, Ng AW, Law EK, Tse WL, Wong CW, Ho PC. Intrinsic carpal ligaments on MR and multidetector CT arthrography: comparison of axial and axial oblique planes. Eur Radiol 2017;27:1277-85.
51. Robinson G, Chung T, Finlay K, Friedman L. Axial oblique MR imaging of the intrinsic ligaments of the wrist: initial experience. Skeletal Radiol 2006;35:765-73.
52. Manton GL, Schweitzer ME, Weishaupt D, Morrison WB, Osterman AL, Culp RW, Shabshin N. Partial interosseous ligament tears of the wrist: difficulty in utilizing either primary or secondary MRI signs. J Comput Assist Tomogr 2001;25:671-6.
53. Shin AY, Battaglia MJ, Bishop AT. Lunotriquetral instability: diagnosis and treatment. J Am Acad Orthop Surg 2000;8:170-9.
54. Gheno R, Buck FM, Nico MA, Trudell DJ, Resnick D. Differences between radial and ulnar deviation of the wrist in the study of the intrinsic intercarpal ligaments: magnetic resonance imaging and gross anatomic inspection in cadavers. Skeletal Radiol 2010;39:799-805.
55. Overstraeten LV, Camus EJ, Wahegaonkar A, Messina J, Tandara AA, Binder AC, Mathoulin CL. Anatomical Description of the Dorsal Capsulo-Scapholunate Septum (DCSS)-Arthroscopic Staging of Scapholunate Instability after DCSS Sectioning. J Wrist Surg 2013;2:149-54.
56. Filippucci E, Gabba A, Di Geso L, Girolimetti R, Salaffi F, Grassi W. Hand tendon involvement in rheumatoid arthritis: an ultrasound study. Semin Arthritis Rheum 2012;41:752-60.
57. Nahra ME, Bucchieri JS. Ganglion cysts and other tumor related conditions of the hand and wrist. Hand Clin 2004;20:249-60, v.
58. Ho PC, Griffiths J, Lo WN, Yen CH, Hung LK. Current treatment of ganglion of the wrist. Hand Surg 2001;6:49-58.
59. Lowden CM, Attiah M, Garvin G, Macdermid JC, Osman S, Faber KJ. The prevalence of wrist ganglia in an asymptomatic population: magnetic resonance evaluation. J Hand Surg Br 2005;30:302-6.
60. Crisco JJ, Chelikani S, Brown RK, Wolfe SW. The effects of exercise on ligamentous stiffness in the wrist. J Hand Surg Am 1997;22:44-8.
61. Goldsmith S, Yang SS. Magnetic resonance imaging in the diagnosis of occult dorsal wrist ganglions. J Hand Surg Eur Vol 2008;33:595-9.
62. Middleton WD, Patel V, Teefey SA, Boyer MI. Giant cell tumors of the tendon sheath: analysis of sonographic findings. AJR Am J Roentgenol 2004;183:337-9.
63. Hung EH, Griffith JF, Ng AW, Lee RK, Lau DT, Leung

JC. Ultrasound of musculoskeletal soft-tissue tumors superficial to the investing fascia. AJR Am J Roentgenol 2014;202:W532-40.

64. Griffith JF. Practical approach to ultrasound of soft tissue tumors and the added value of MRI: how I do it. J Ultrason 2023;23:e299-312.

Cite this article as: Ng AWH, Chan JYS, Griffith JF, Ng ISH, Tse WL, Ng SSH. Imaging of dorsal wrist pain. Quant Imaging Med Surg 2024;14(9):6945-6962. doi: 10.21037/qims-24-420